

## Quantification of Effective Flow Resistivity for Parametric Assessment of Pervious Concrete by Using Ultrasonic Pulse Velocity Method

Singh, Avishreshth; Biligiri, Krishna Prapoorna; Sampath, Prasanna Venkatesh

**DOI**

[10.1177/03611981231160175](https://doi.org/10.1177/03611981231160175)

**Publication date**

2023

**Document Version**

Final published version

**Published in**

Transportation Research Record

**Citation (APA)**

Singh, A., Biligiri, K. P., & Sampath, P. V. (2023). Quantification of Effective Flow Resistivity for Parametric Assessment of Pervious Concrete by Using Ultrasonic Pulse Velocity Method. *Transportation Research Record*, 2677(10), 64-78. <https://doi.org/10.1177/03611981231160175>

**Important note**

To cite this publication, please use the final published version (if applicable). Please check the document version above.

**Copyright**

Other than for strictly personal use, it is not permitted to download, forward or distribute the text or part of it, without the consent of the author(s) and/or copyright holder(s), unless the work is under an open content license such as Creative Commons.

**Takedown policy**

Please contact us and provide details if you believe this document breaches copyrights. We will remove access to the work immediately and investigate your claim.


***Green Open Access added to TU Delft Institutional Repository***

***'You share, we take care!' - Taverne project***

**<https://www.openaccess.nl/en/you-share-we-take-care>**

Otherwise as indicated in the copyright section: the publisher is the copyright holder of this work and the author uses the Dutch legislation to make this work public.

# Quantification of Effective Flow Resistivity for Parametric Assessment of Pervious Concrete by Using Ultrasonic Pulse Velocity Method

Transportation Research Record  
2023, Vol. 2677(10) 64–78  
© National Academy of Sciences:  
Transportation Research Board 2023  
Article reuse guidelines:  
sagepub.com/journals-permissions  
DOI: 10.1177/03611981231160175  
journals.sagepub.com/home/trr  


Avishreshth Singh<sup>1</sup> , Krishna Prapoorna Biligiri<sup>2</sup> , and Prasanna Venkatesh Sampath<sup>2</sup>

## Abstract

The use of nondestructive ultrasonic pulse velocity (UPV) testing to assess the hardened properties of pervious concrete (PC) mixtures is an emerging research area. Further, UPV has been successfully used to determine the effective flow resistivity (EFR) of asphalt concrete and cement concrete pavements. However, no research studies have focused on understanding PC characteristics using EFR. Thus, the major objectives of this study were to assess the suitability of UPV testing for characterizing PC mixtures and to quantify their EFR, which is a measure of the material's characteristic impedance and is dependent on the mix variables along with porosity. Thirty-six control and sand-modified PC mixtures were prepared with four aggregate gradations, and three levels each of water-to-cement (*w/c*) and aggregate-to-cement (*a/c*) ratios. Test results indicated that EFR was significantly dependent on the mix variables, with aggregate gradation being the most influential factor (six and eight times higher than *w/c* and *a/c* ratios, respectively). Lower EFR or higher sound absorption capacity was reported for PC with higher porosities. The sand-modified PC mixtures had higher EFR (by 4%–12%) than the control PC, and consequently lower sound absorption capacity, attributed to the presence of mortar that densified the mixes. Further, good-to-excellent correlations were obtained for various PC properties with UPV and EFR, which underscored the potential of UPV in characterizing PC. The major contribution of this research was the development of a simple, fast, and cost-effective approach, which can be suitably adopted as a quality-control test to determine PC mixture properties.

## Keywords

Pervious concrete, ultrasonic pulse velocity, effective flow resistivity, dynamic modulus of elasticity, material properties, nondestructive tests

During the last few decades, researchers across the world have shown keen interest in developing sustainable pavement materials and infrastructure that have the potential to mitigate several challenges in urban areas such as flash floods, elevated temperatures, and tire–pavement interaction noise. Pervious concrete (PC) is one such sustainable material that is designed by careful proportioning of coarse aggregates and cement to create a gap-graded pore network structure (1, 2). Though PC has been recognized for its stormwater infiltration ability, it also provides several other advantages over conventional pavements, such as improved resistance to skidding and hydroplaning,

limited material requirement (e.g., no or limited sand), and lower tire–pavement noise (3–6).

PC is typically characterized by its high porosity and low compressive strength, which restricts its

<sup>1</sup>Section of Pavement Engineering, Faculty of Civil Engineering and Geosciences, Delft University of Technology, The Netherlands

<sup>2</sup>Department of Civil & Environmental Engineering, Indian Institute of Technology Tirupati, Andhra Pradesh, India

## Corresponding Author:

Avishreshth Singh, avi.theriac@gmail.com; avi.singh@tudelft.nl; ce18d001@iittp.ac.in

implementation in areas with low-to-medium traffic, medians, and highway shoulders (7, 8). Researchers have used different test methods to evaluate the pore parameters and performance characteristics of PC. For instance, the porosity and density are typically computed using material science theories, vacuum method, and image analysis (9–12). Similarly, the permeability is quantified by performing falling and/or constant head tests, while destructive testing is commonly utilized to evaluate the strength of PC (13). With recent technological advances, some researchers have also focused on utilizing simple and cost-effective nondestructive methods such as ultrasonic pulse velocity (UPV) (14–16), which is commonly used to assess the quality of traditional concrete. A study showed that the correlations between UPV and PC characteristics were not very strong (17), while others have reported that UPV presents fairly strong correlations with PC properties (16). Another piece of research proposed statistical models to predict the compressive strength and hydraulic conductivity of PC (18). Nonetheless, more research is required that can encompass a vast range of mix variables.

With respect to skid resistance, researchers have reported that the PC surface wearing course layers offer higher friction than conventional pavements, thereby having a high potential to minimize skidding-induced accidents (19). Moreover, the porous structure of PC acts as a dampening medium for sound and can reduce the tire–pavement noise by 3 to 5 dB compared with conventional pavements, attributed to the high porosity and interconnected pore network (20). An investigation suggested that the sound absorption capability of PC was higher than that of porous asphalt, with sound absorption coefficients of 0.1% to 20% greater under clogged and unclogged conditions, respectively (5). It has been found that the sound absorption in PC is a function of aggregate size and gradation, paste content, porosity, pore size and distribution, and specimen size, along with other factors such as air humidity (21–23). In general, the sound absorption characteristics of PC and other pavement types or the tire–pavement interaction noise have been investigated using the standing wave method, onboard sound intensity method, and impedance tube (5, 21, 24).

In the past, researchers recommended the use of effective flow resistivity (EFR), which is the measure of acoustic impedance of a material, to determine the tire–pavement noise (25–28). The EFR depends on the material parameters such as porosity, tortuosity, pore distribution, and thickness (26, 28). Typically, the EFR values for conventional pavement types such as asphalt concrete, aged asphalt concrete, and cement concrete have been estimated to be 5000 to 15,000 cgs Rayls, 30,000 cgs Rayls, and 20,000 cgs Rayls, respectively (28). The EFR

is generally determined by measuring the difference in the sound pressure levels for frequencies ranging between 250 and 4000 Hz (29). However, a few investigations have proposed a simplified framework to evaluate the impedance or EFR of several asphalt concrete mixtures (laboratory and field cores) using the UPV test method (25, 26). It was suggested that for waves measured within the sonic range, the frequency had a significant effect, while frequency was not deemed important in the case of the ultrasonic range (26). A predictive model was also proposed based on the transit time without considering the pore arrangement within the mix matrix. Further, the EFR was found to have a strong correlation with the tire–pavement noise data gathered in the field using the onboard sound intensity method and noise meter. Thus, it was recommended that the UPV method is well suited to predicting the EFR or characteristic fundamental impedance of paving mixtures.

Based on the past literature, it was clear that though investigations on the use of UPV to determine the PC properties are emerging, there still exists significant room to investigate additional mixtures, with sand being one of the variables. Further, several methods have been employed in the past to study the sound absorption characteristics of PC mixtures by utilizing expensive instrumentation and analytical tools. In addition, it was also understood that though EFR has been used in the past to quantify the impedance of asphalt concrete mixtures (open-graded asphalt, porous asphalt, and dense-graded asphalt), there have not been systematic studies that have focused on the utilization of EFR as a parameter to understand the hardened properties (porosity, density, permeability, and compressive strength) of PC mixtures and their impedance, which is also an indirect measure of the porosity/density of a material as well as being an acoustic property assessor.

Therefore, the primary objective of this first-of-its-kind research was to explore the potential of utilizing the nondestructive UPV test to ascertain the EFR of control and sand-modified PC mixtures. The influence of mix variables and other hardened properties of PC on the EFR were investigated through the UPV test technique along with assessing the quality of mixtures through statistical inference. It is envisioned that the simplified approach proposed in this study can be adopted as a nondestructive quality control test to characterize the physical, hydrological, and mechanical properties of PC mixtures. Furthermore, tire–pavement noise is a function of the porosity of any paving mix, as demonstrated by several investigations and expert opinions (5, 20, 21, 23). Therefore, it is anticipated that the impedance or EFR of PC will provide important information that could be utilized to conduct acoustic studies based on material inputs in the future.

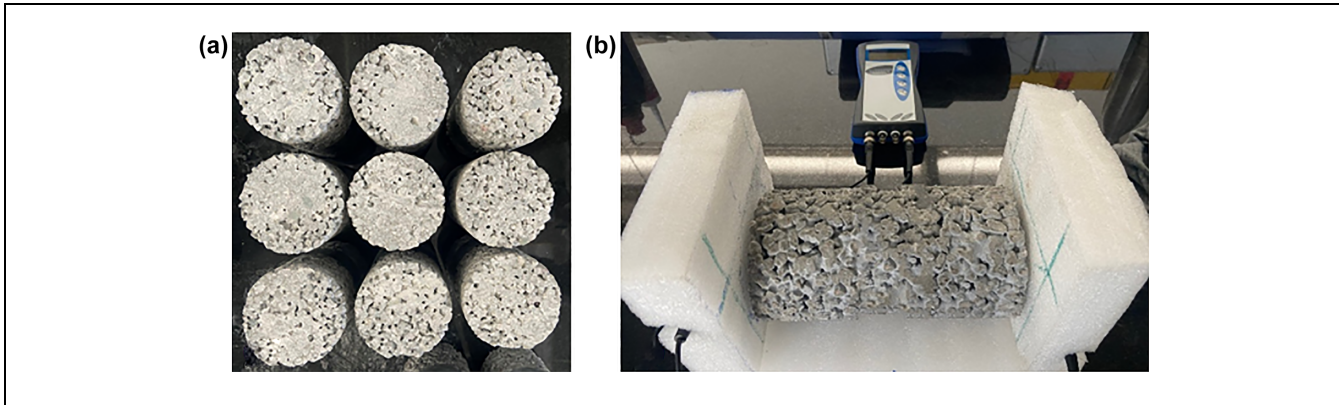


**Figure 1.** Ultrasonic pulse velocity measurements: (a) trimmed pervious concrete specimens, and (b) test setup.

## Materials and Methodology

In this research, a full factorial experimental design was undertaken to examine 36 PC mixtures having two control and two sand-modified gradations each, which were designated as:

- G-1: 9.5–6.3 mm,
- G-2: 6.3–4.75 mm,
- G-1S: 9.5–6.3 mm + 10% fines, and
- G-2S: 6.3–4.75 mm + 10% fines.

Sand was added as a partial replacement of coarse aggregates (10% by weight). Further, three levels of water-to-cement (w/c) (0.27, 0.30, and 0.33) and aggregate-to-cement (a/c) (3.75, 4.00, and 4.25) ratios were adopted. In addition, a superplasticizer was added in the proportion of 0.25% by cement mass (30). The aggregate properties conformed to Indian Standard (IS) 2386 (31), while Ordinary Portland cement 53 grade met the requirements of IS 12269 (32), as reported in published documents (33, 34). Three replicate specimens (100 mm × 200 mm) were prepared per mix type resulting in a total of 108 cylinders, and the detailed experimental matrix encompassing the various mix proportions is presented elsewhere (33). The specimens were compacted in two layers by providing 25 blows on each layer with a standard Proctor hammer (9, 33).

### Hardened Density and Porosity

The hardened density and porosity of PC specimens were determined in accordance with ASTM C1754 (35). The detailed procedure is described in the literature as well (33).

### Permeability

The permeability of PC cylinders was estimated based on Darcy's principle as per the procedure described in the literature (33).

### Ultrasonic Pulse Velocity and Dynamic Modulus of Elasticity

The UPV test was performed in accordance with ASTM C597 (36), and the time taken for the propagation of longitudinal ultrasonic pulse through the PC was noted. The test setup comprised a pulse generator connected to two electro-acoustical transducers: (a) a transmitter that helped in the generation of longitudinal stress waves, and (b) a receiver that collected and converted the ultrasonic pulse into an electrical signal.

Before the measurement of pulse velocity, the top 10 mm of each of the PC specimens was trimmed with a concrete cutter to attain a relatively smooth surface and ensure uniform contact between transducers and PC (Figure 1a). Figure 1b presents the setup used for performing the experiment. The faces of transducers and PC cylinders were coupled by applying petroleum jelly, which guaranteed a voidless contact and consistent energy transfer between the specimens and transducers. In this study, a transducer set with a frequency range of 55 kHz was used.

Once the pulse velocity was determined, attempts were made to quantify the dynamic modulus of elasticity (DME) of the PC mixtures (17, 36). DME is an important parameter that governs the stiffness of a material. Since limited studies have focused on understanding the modulus of PC and its relationship with material properties such as compressive strength, an effort was made to determine the DME using pulse velocity (from the UPV test) and Poisson's ratio as the major inputs. Although a previous study suggested that the range of Poisson's ratio varies from 0.23 to 0.27 (17), this research made an effort to investigate this parameter for the given set of mixtures in a similar manner. However, a broader range of Poisson's ratios (0.15, 0.18, 0.21, 0.24, 0.27, and 0.30) was used in this study. Analysis of variance (ANOVA) and post hoc tests were performed to investigate the significant differences in dynamic moduli computed using

six Poisson's ratios. The ANOVA test results revealed that Poisson's ratios had a significant effect on the dynamic moduli, but Sidak's post hoc test results indicated that dynamic moduli were not significantly different at 95% confidence level for Poisson's ratios of 0.18, 0.21, and 0.24 (37). Therefore, the Poisson's ratio was assumed as 0.24.

### Unconfined Compressive Strength

The unconfined compressive strength (UCS) was calculated on capped PC cylinders by applying load in a stress-controlled mode at a rate of 1 MPa/min (38). Since PC is a highly porous material with an interconnected pore network structure, a slow rate of loading was used to prevent the samples from being subjected to sudden loading, which may otherwise have led to premature failure.

### Effective Flow Resistivity

The impedance of the PC mixtures was computed using the relationship given in Equation 1 and is expressed in Newton-seconds per cubic meter. The impedance computed by the product of density and UPV is representative of a material's mechanical impedance per unit area, which is also referred to as the EFR (25, 26). Note that EFR is a measure of the material's characteristic impedance and not a specific acoustic impedance. Therefore, the impedance derived for the different PC mixtures may also be used as a direct input in the Federal Highway Administration's traffic noise model for investigations pertaining to noise abatement designs (29). The EFR can also be expressed in the units of cgs Rayls by multiplying the resultant obtained from Equation 1 by a factor of 0.10.

$$Z = \rho \times v \quad (1)$$

where

- $Z$  = impedance in N.s/m<sup>3</sup>,
- $\rho$  = density of the material in kg/m<sup>3</sup>, and
- $v$  = UPV through the material in m/s.

## Results

### Hardened Density and Porosity

On average, the hardened porosity and density of the PC mixtures varied from 21% to 32% and from 1704 to 1927 kg/m<sup>3</sup>, respectively, while those for sand-modified mixtures were in the range of 19% to 30% and 1824 to 2031 kg/m<sup>3</sup>, respectively. Further, the respective coefficients of variation for porosity and density varied from 0.54% to 11% and 0.15% to 2.51% for control PC

mixtures, and 0.40% to 14.95% and 0.24% to 5.03% for PC with sand. Figure 2, *a* to *d*, presents the influence of varying w/c and a/c ratios for different aggregate gradations on porosity and density.

Regardless of the inclusion of sand, the density of mixtures prepared with small-sized aggregates was lower; this was attributed to their higher surface area, which required more paste content to coat the aggregates for a given volume of the mix (33, 37). Further, the large-sized aggregates were less angular (about 40%) than small-sized aggregates, indicative of their ability to undergo a higher degree of compaction, resulting in lower porosity and higher density. The porosity of gradations G-1S and G-2S was lower, while their density was higher compared with G-1 and G-2; this is ascribed to the addition of sand, which filled the pore spaces in the PC (33). Additionally, an increase in the w/c ratio resulted in the production of mixtures with lower porosity and higher density. This was attributed to the availability of higher paste content, which made the mix more workable and further allowed the migration of paste into the pores of the PC after coating the aggregate particles. Moreover, as the a/c ratio increased, the density of PC reduced with an increase in the porosity resulting from the greater total volume of aggregates for a given mixture, which led to the creation of higher numbers of pore channels. Furthermore, an increase in porosity reflected a reduction in density, which corroborated with the previously reported literature (39, 40).

### Permeability

The permeability of PC mixtures with and without sand varied from 0.27 to 1.11 cm/s and 0.22 to 0.60 cm/s, respectively. Further, the coefficients of variation varied from 0.01% to 0.25% for PC mixtures without sand, and 0.04% to 0.53% for PC mixes with sand. Figure 3 depicts the respective influence of different aggregate gradations with varying w/c and a/c ratios on the permeability of PC mixtures. As can be observed from Figure 3*a*, the permeability decreased with an increase in the w/c ratio; this is attributed to the availability of higher paste volume, which not only coated the aggregates but also occupied the pores (33). Further, the variations in permeability for G-1S and G-2S followed a similar trend as that for porosity. Note that the incorporation of sand in PC augmented the binding area, thereby densifying the mixtures and resulting in lower permeability (41, 42). In general, an increase in the aggregate content for a given paste or mortar volume resulted in the production of mixtures with higher permeability (Figure 3*b*), ascribed to the increased surface area, which was a result of the availability of lower cement content for occupying the interstices within the PC (33).

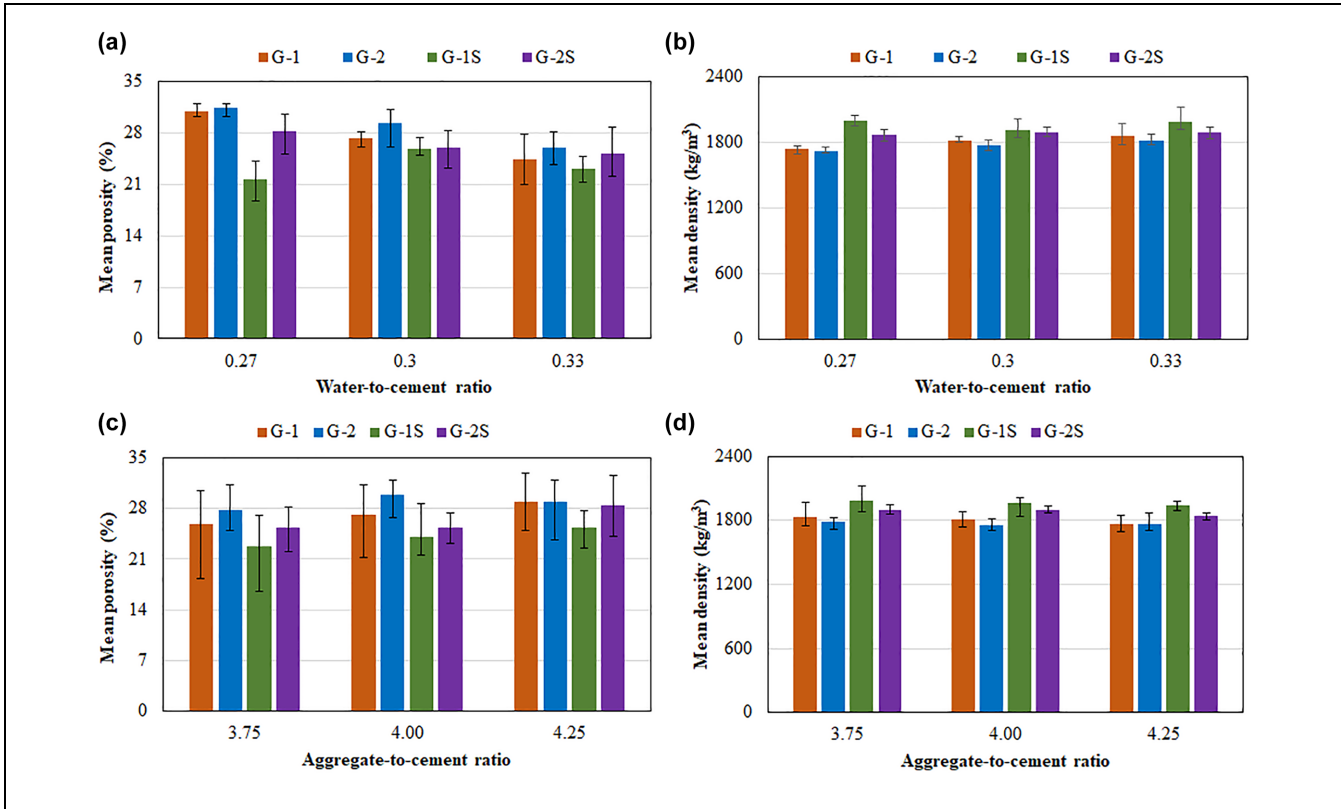


**Figure 2.** Influence of varying aggregate gradations and increasing: (a) water-to-cement ratio on porosity, (b) water-to-cement ratio on density, (c) aggregate-to-cement ratio on porosity, and (d) aggregate-to-cement ratio on density. Note: G-1, G-2, G-1S, and G-2S represent the two control and two sand-modified (S) aggregate gradations.

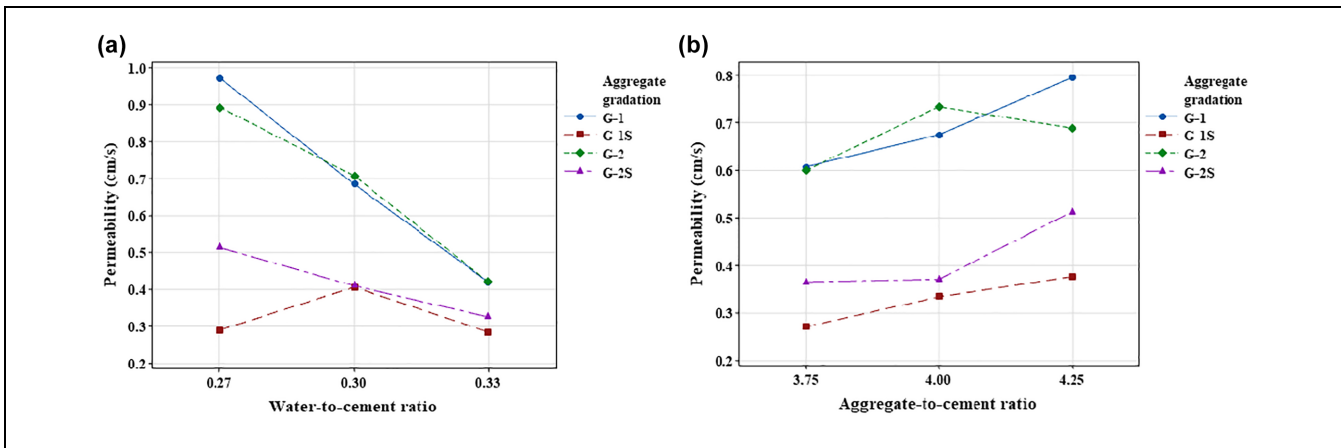


**Figure 3.** Influence of varying aggregate gradations on the permeability of pervious concrete with increasing: (a) water-to-cement ratio and (b) aggregate-to-cement ratio.

*Statistical Distributions.* In this study, the permeability data were best represented by the three-parameter Weibull distribution, and the distribution parameters were fitted using the distribution identification function in Minitab® software. The major function of a PC sample is to allow

rapid infiltration of stormwater, which is attributed to the high void ratio (or porosity). Therefore, PC must always have a minimum rate of permeability to serve its intended function, which may be represented by the location parameter ( $\gamma$ ). Further, the permeability of PC tends to reduce

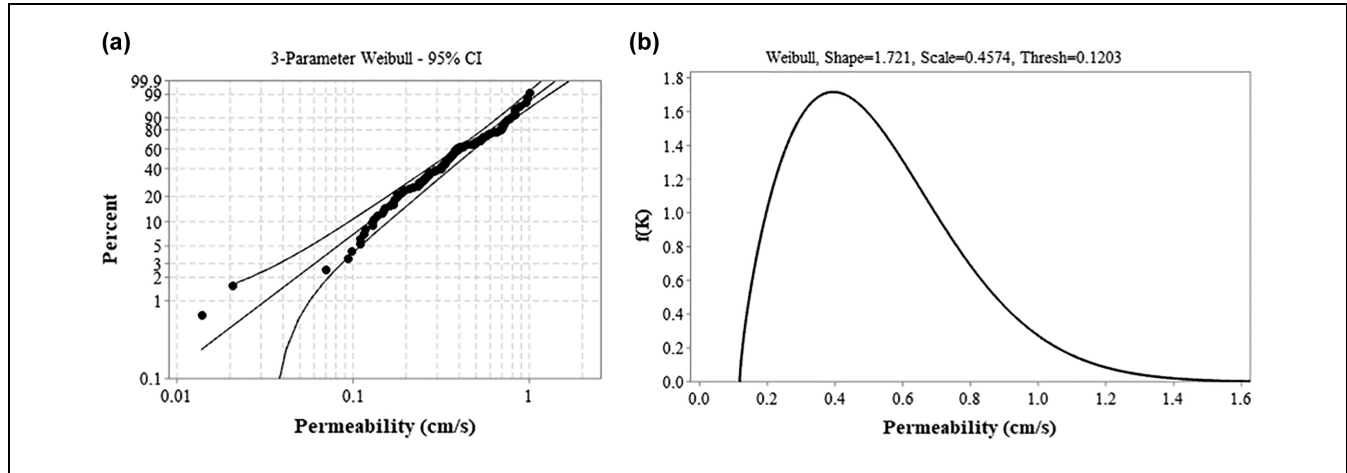


**Figure 4.** Three-parameter Weibull distribution for permeability: (a) probability plot, and (b) probability distribution function. Note: CI = confidence interval; thresh = threshold.

over time because of the clogging of the porous network structure. Therefore, the reduction in permeability may be represented by the shape parameter ( $\beta$ ). Finally, the range of permeability values may be described by the scale parameter ( $\eta$ ). The general expression for the three-parameter Weibull distribution is given in Equation 2, and the fitted distribution function ( $K_p$ ) is given in Equation 3. The probability plot and Weibull distribution function are presented in Figure 4, *a* and *b*, respectively.

$$f(K_p) = \frac{\beta}{\eta} \times \left( \frac{K_p - \gamma}{\eta} \right)^{\beta-1} \times e^{-\left( \frac{K_p - \gamma}{\eta} \right)^\beta} \quad (2)$$

where

- $K_p$  = permeability in cm/s,
- $\beta$  = shape parameter,
- $\gamma$  = location parameter, and
- $\eta$  = scale parameter.

$$f(K_p) = \frac{1.721}{0.457} \times \left( \frac{K_p - 0.120}{0.457} \right)^{0.721} \times e^{-\left( \frac{K_p - 0.120}{0.457} \right)^{1.721}} \quad (3)$$

### Ultrasonic Pulse Velocity and Dynamic Modulus of Elasticity

The UPV of control and sand-modified PC mixtures varied from 3296.74 to 4524.82 m/s and from 3551.02 to 4508.24 m/s, respectively. In addition, the DME for control and sand-modified PC mixtures ranged from 15.75 to 34.23 GPa and from 19.31 to 34.97 GPa, respectively. The variations of UPV and DME with increasing w/c and a/c ratios are presented in Figure 5, *a* to *d*, respectively. Further, ANOVA showed that all three independent

variables (aggregate gradation, w/c ratio, and a/c ratio) and their three-way interactions had significant effects on the UPV and DME, as summarized in Table 1. The relative contribution of aggregate gradation was found to be the highest, whereas w/c and a/c ratios had lower effects.

In general, it was observed from Figure 5, *a* to *d*, that PC mixtures prepared with gradations G-1 and G-1S had higher UPV and DME than did their respective counterparts G-2 and G-2S. This may be explained as follows:

- G-2 and G-2S gradations comprised more angular particles (angularity number of 9.65) compared with G-1 and G-1S (angularity number of 5.76), which provided higher aggregate interlock. As a result, more resistance was offered to compaction by gradations G-2 and G-2S leading to the development of PC mixtures with lower density.
- For a given volume of the mixture, the number of particles in gradations G-2 and G-2S was plausibly higher than G-1 and G-1S, thereby requiring more cement paste to coat the aggregates and producing more porous mixtures.
- An increase in the a/c ratio resulted in mixtures with increased porosity and consequently lower density that might have caused a reduction in UPV and DME of PC.
- An increase in the w/c ratio led to an increase in density, which may be attributed to the higher workability that provided a thicker coating of cement paste/mortar over the aggregates and also occupied some additional pores, resulting in higher magnitudes of pulse velocity and dynamic modulus.

Furthermore, for sand-modified mixtures, higher UPV and DME were observed for mixtures with higher



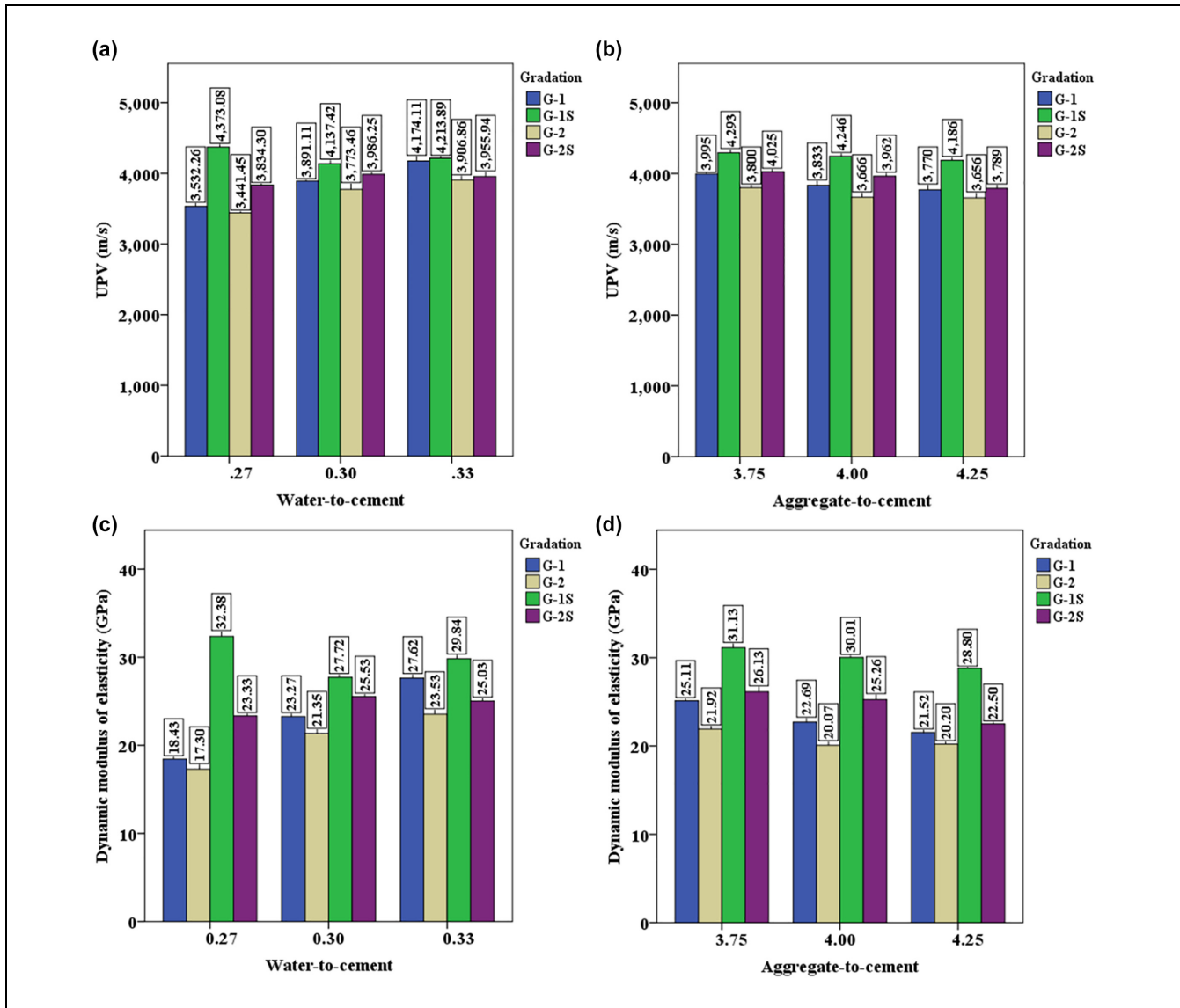


**Figure 5.** Influence of varying aggregate gradations and: (a) water-to-cement ratio on ultrasonic pulse velocity (UPV), (b) aggregate-to-cement ratio on UPV, (c) water-to-cement ratio on dynamic modulus of elasticity (DME), and (d) aggregate-to-cement ratio on DME.

densities and lower porosities. This further corroborated the discussion mentioned above, which suggests that higher UPV and DME are achievable for PC with higher density. The relationships between UPV, DME, and other hardened properties of PC are illustrated using scatter plots in Figure 6, *a* to *g*. Good-to-excellent correlations were observed between the different parameters, highlighting the potential of using UPV as a quality-control non-destructive test method to evaluate PC mixtures.

### Unconfined Compressive Strength

The average UCS of PC cylinders tested in this study was found to vary from 8.24 to 21.37 MPa for mixtures without sand, and from 14.48 to 32.93 MPa for sand-modified

PC mixtures. The influence of varying *w/c* and *a/c* ratios on different aggregate gradations is presented in Figure 7, *a* and *b*, respectively.

The mixtures prepared with gradations G-1 and G-1S showed higher UCS than did their counterpart mixtures with gradations G-2 and G-2S. This was attributed to their lower porosity, which indicated the higher effective spacing between the pores that would reduce their early encounter with the stress path, leading to higher strength (43). In addition, the sand-modified PC mixtures resulted in higher strength, ascribed to their higher density than the control PC (33). An increase in *w/c* ratio was consequential of mixtures with greater UCS except for gradation G-2S, attributed to the random distribution of pores in the PC, which might have caused an early encounter

**Table 1.** Summary of Analysis of Variance Results for Ultrasonic Pulse Velocity and Dynamic Modulus of Elasticity

Dependent variable	Source	Type III sum of squares	Degree of freedom	Mean square	F	Sig.
Ultrasonic pulse velocity (m/s)	Gradation	4,067,868.97	3	1,355,956.32	202.95	< 0.05
	w/c	1,295,178.22	2	647,589.11	96.92	< 0.05
	a/c	572,687.50	2	286,343.75	42.86	< 0.05
	Gradation * w/c	1,977,796.73	6	329,632.79	49.34	< 0.05
	Gradation * a/c	105,403.81	6	17,567.30	2.63	0.023
	w/c * a/c	125,380.62	4	31,345.15	4.69	< 0.05
	Gradation * w/c * a/c	360,929.91	12	30,077.49	4.50	< 0.05
	Residual	481,057.06	72	6681.35		
	Total	8,986,302.81	107			
Dynamic modulus of elasticity (GPa)	Gradation	1245.86	3	415.29	253.07	< 0.05
	w/c	240.32	2	120.16	73.23	< 0.05
	a/c	143.78	2	71.89	43.81	< 0.05
	Gradation * w/c	441.90	6	73.65	44.88	< 0.05
	Gradation * a/c	25.31	6	4.22	2.57	0.03
	w/c * a/c	28.66	4	7.17	4.37	< 0.05
	Gradation * w/c * a/c	101.46	12	8.45	5.15	< 0.05
	Residual	118.15	72	1.64	na	na
	Total	2345.44	107	na	na	na

Note: Sig. = significance; w/c = water-to-cement ratio; a/c = aggregate-to-cement ratio; na = not applicable.

with the stress path. Further, the density of PC mixtures was lower at higher aggregate content for a given paste/mortar volume, and consequently, their corresponding UCS was lower.

Figure 8, *a* and *b*, presents the correlations between UCS and other measured parameters of UPV. Interestingly, strong correlations were observed between UCS and UPV parameters, where UCS increased with increasing UPV and DME. These findings were found to be crucial since a nondestructive technique such as UPV exhibited excellent potential in predicting UCS and DME, the latter being a critical variable that could be cogently used in the pavement design process.

**Statistical Distributions.** The UCS data were fitted by a three-parameter Weibull distribution function. To be a suitable candidate for pavement applications and perform satisfactorily over its design life, PC must possess minimum strength, which was represented by  $\gamma$  (minimum strength parameter). Further, the compressive strength of PC deteriorates with time when subjected to repeated vehicular loads because of the development of strains within the mix, represented by  $\beta$ . The data values may be described by  $\eta$ . The fitted three-parameter Weibull distribution function is given in Equation 4. Further, the probability plot (along with the goodness-of-fit statistics) and Weibull distribution function are shown in Figure 9, *a* and *b*, respectively. The Anderson–Darling (A-D) statistics for normal, lognormal, and gamma distributions were 1.226, 0.402, and 0.364, respectively. Although the A-D value for lognormal was lower than the three-

parameter Weibull, it was not suitable, as the data obtained after taking the natural log of the original UCS data did not follow a normal distribution. Further, gamma distribution was not logical as it did not provide a cutoff point based on the dataset, and lower values were also likely, which would lead to the production of very low-strength PC mixtures unsuitable for field applications.

$$f(\text{UCS}) = \frac{1.610}{10.506} \times \left( \frac{\text{UCS} - 7.325}{10.506} \right)^{0.610} \times e^{-\left( \frac{\text{UCS} - 7.325}{10.506} \right)^{1.610}} \quad (4)$$

### Effective Flow Resistivity

The EFR was found to vary from 5517 to 8739 cgs Rayls and from 6279 to 9072 cgs Rayls for control and sand-modified PC mixtures, respectively, and the corresponding coefficients of variation ranged from 0.86% to 4.55% and from 0.48% to 7.27%. ANOVA test results (Table 2) revealed that the individual contributions of the three mix variables as well as the two-way and three-way interactions were significant ( $p < 0.05$ ). The plots for the main effects (Figure 10) showed that the aggregate gradation was the major parameter that governed the EFR parameter followed by w/c and a/c ratios. The individual contribution of the mix variables was computed as the ratio of the sum of squares of a factor to the total sum of squares for all the factors. It was found that the contribution of aggregate gradation was about 6 and 10 times higher than that of the w/c ratio and a/c ratio,

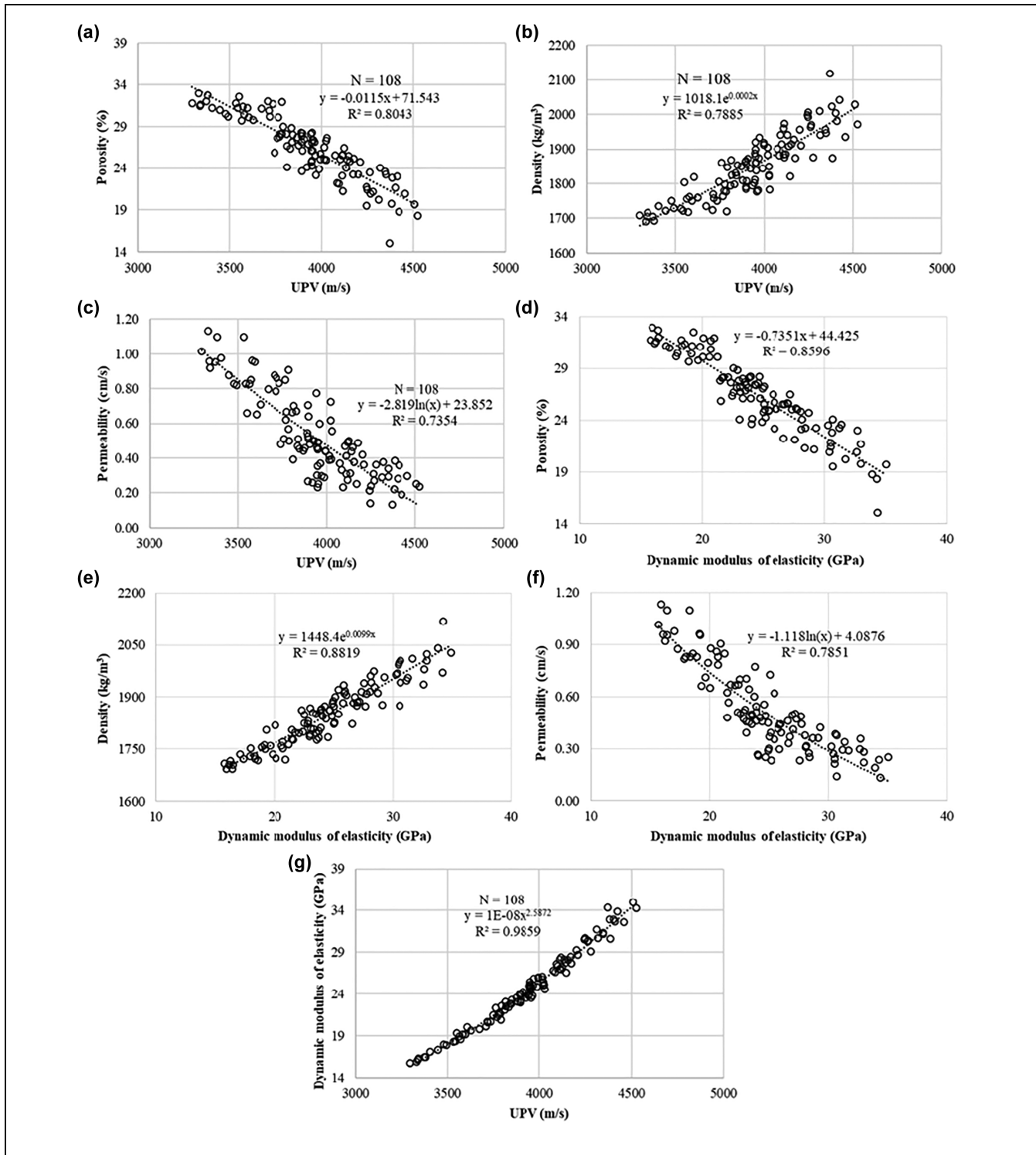


**Figure 6.** Correlations between: (a) ultrasonic pulse velocity (UPV) and porosity, (b) UPV and density, (c) UPV and permeability, (d) dynamic modulus of elasticity (DME) and porosity, (e) DME and density, (f) DME and permeability, and (g) UPV and DME.

respectively. This finding also suggested that the aggregate gradation governed the pore arrangement, which in

turn had a significant effect on the EFR parameter through the PC material (24, 33).

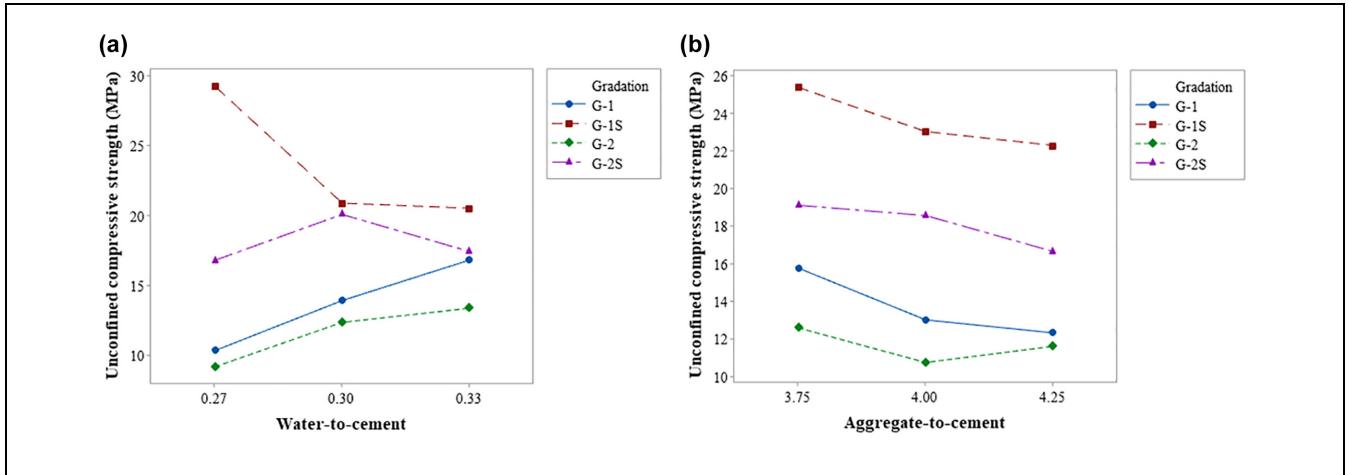


**Figure 7.** Influence of varying aggregate gradations and: (a) water-to-cement ratio on unconfined compressive strength (UCS), and (b) aggregate-to-cement ratio on UCS.

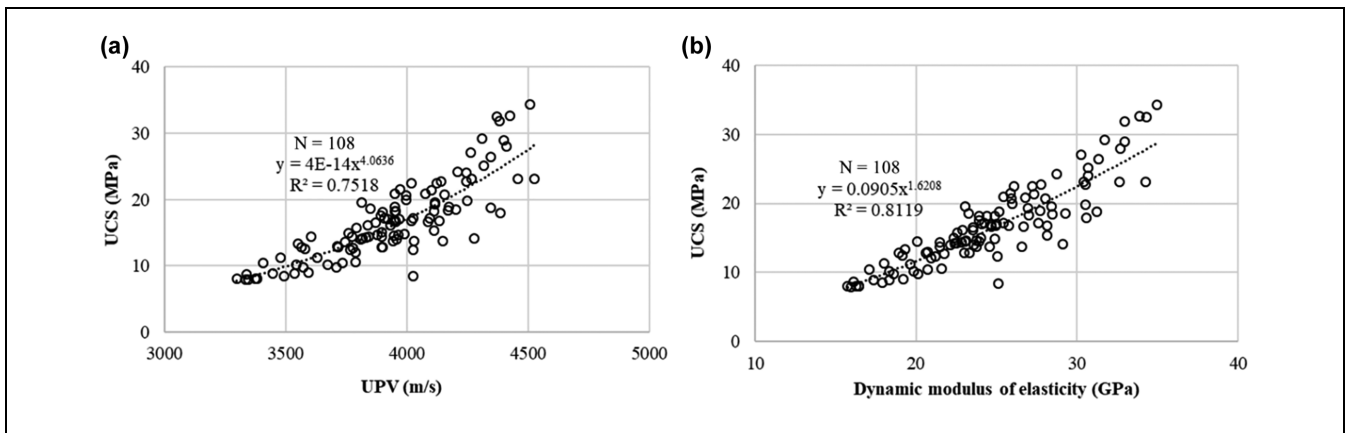


**Figure 8.** Correlations between unconfined compressive strength (UCS) and: (a) ultrasonic pulse velocity (UPV), and (b) dynamic modulus of elasticity.

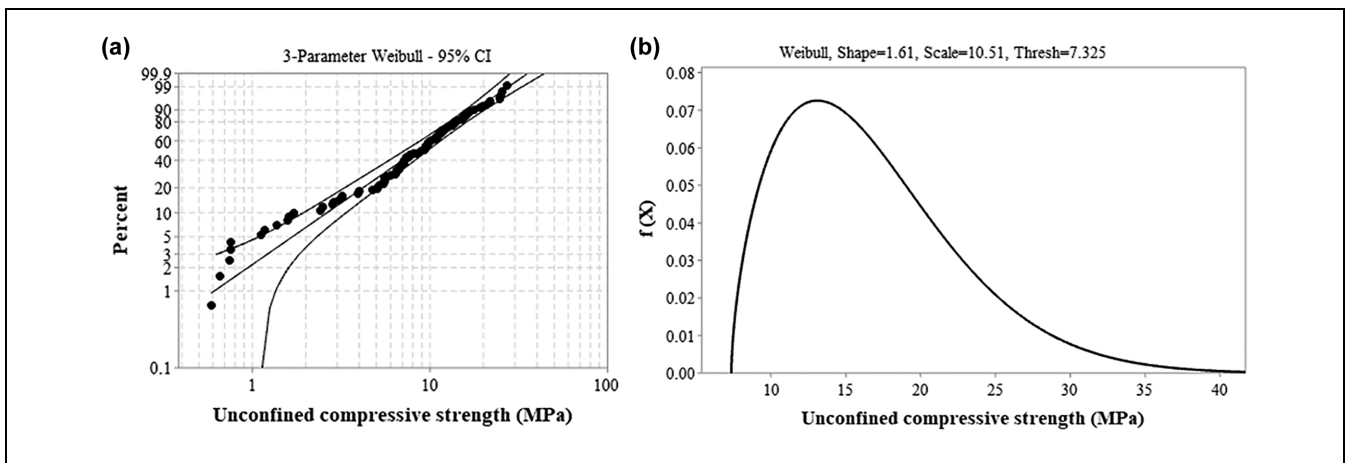


**Figure 9.** Three-parameter Weibull distribution for unconfined compressive strength: (a) probability plot, and (b) probability distribution function.

Note: CI = confidence interval; thresh = threshold.

**Table 2.** Summary of Analysis of Variance Results for Effective Flow Resistivity of Pervious Concrete Mixtures

Dependent Variable	Source	Type III sum of squares	Degree of freedom	Mean square	F	Sig.
Effective Flow Resistivity (cgs Rayls)	Gradation	43,913,175	3	14,637,725	269.57	< 0.05
	w/c	7,955,432	2	3,977,716	73.25	< 0.05
	a/c	4,480,900	2	2,240,450	41.26	< 0.05
	Gradation * w/c	13,288,543	6	2,214,757	40.79	< 0.05
	Gradation * a/c	835,276	6	139,213	2.56	0.023
	w/c * a/c	792,058	4	198,015	3.65	< 0.05
	Gradation * w/c * a/c	3,212,178	12	267,682	4.93	< 0.05
	Residual	3,909,581	72	54,300	na	na
Total	78,387,144	107	na	na	na	

Note: Sig. = significance; w/c = water-to-cement ratio; a/c = aggregate-to-cement ratio; na = not applicable.

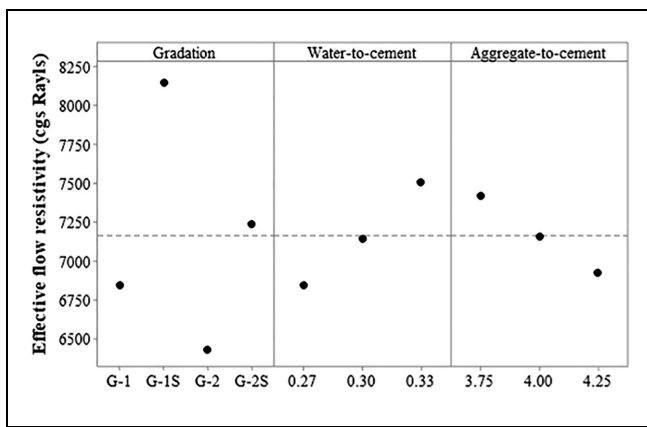


**Figure 10.** Mean effective flow resistivity (cgs Rayls) of pervious concrete mixtures with respect to materials properties.

As observed from Figures 10 and 11, the EFR was lower for sand-modified PC than for the control mixtures, majorly attributed to the inclusion of sand in the matrix, which caused densification of the mix, thereby

resulting in lower porosity and higher density. Further, it is interesting to mention that mixtures designed with small aggregate particles (G-2 and G-2S) that were more angular in nature resulted in higher EFR compared with G-1 and G-1S, attributed to their lower porosities. Other researchers also reported that PC mixtures designed with smaller aggregate sizes had pores with lower sizes, which resulted in a higher sound absorption coefficient, attributed to the presence of a greater number of internal channels for sound propagation (24, 44).

In addition, the EFR increased linearly with increasing w/c ratios, which was indicative of higher tire-pavement noise levels, ascribed to the presence of augmented paste content and the lower porosity of the mix. A similar study reported that the sound absorption coefficient of PC reduced for higher paste content (45). Moreover, higher a/c ratios indicated the presence of a greater number of aggregates for a given mix volume, which utilized greater cement content for coating, concomitant with higher porosity, and better sound absorption characteristics (lower tire-pavement noise) as also reflected by the lower EFR magnitudes. This observation

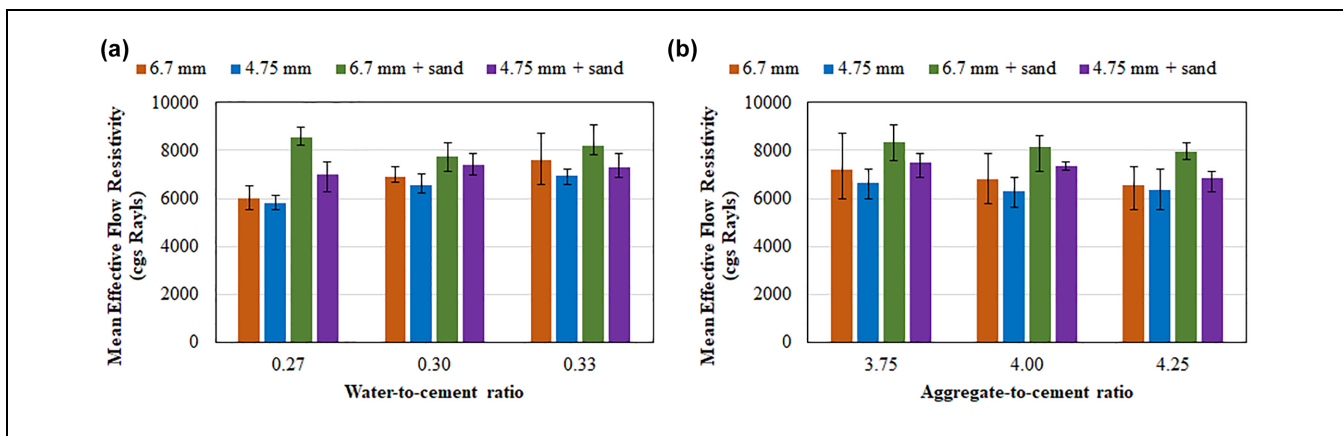


**Figure 11.** Variation in effective flow resistivity (cgs Rayls) with respect to aggregate gradation: (a) water-to-cement ratio, and (b) aggregate-to-cement ratio.

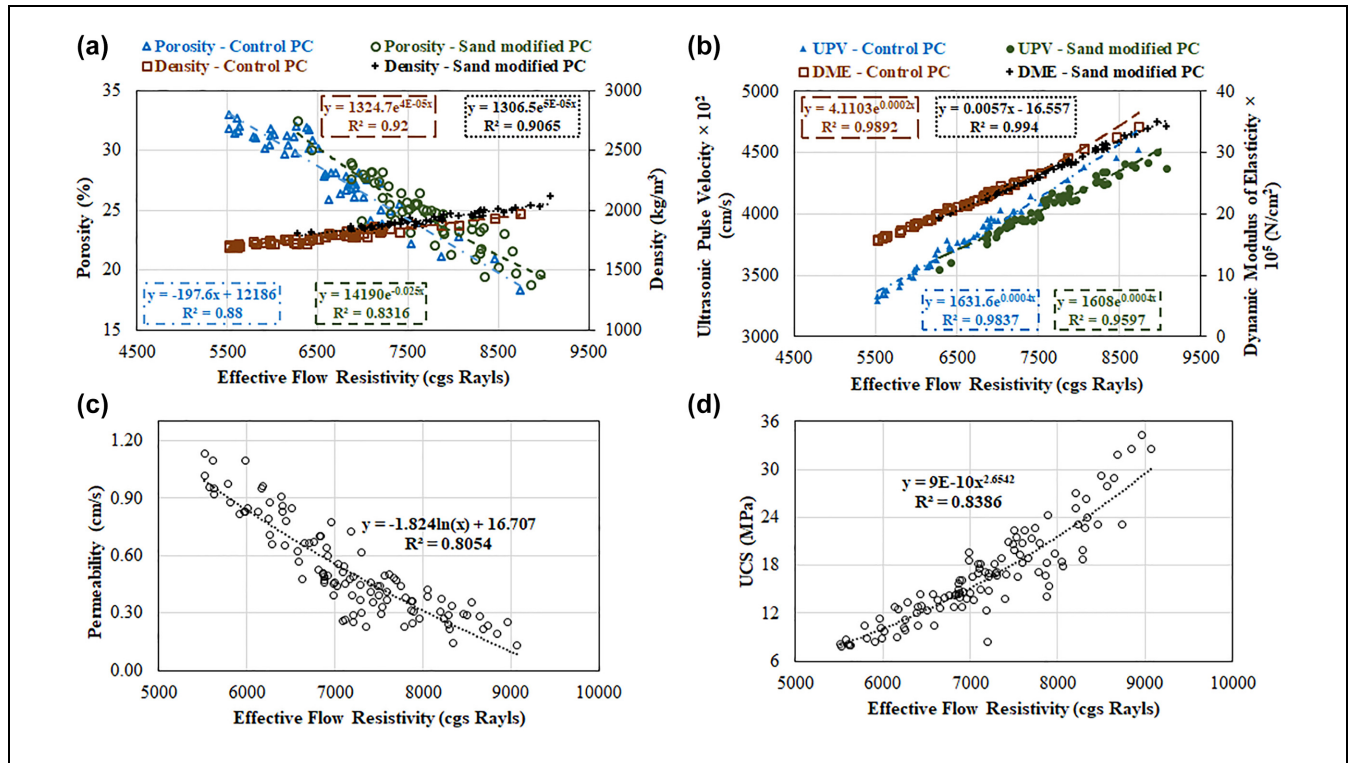


**Figure 12.** Relationship between effective flow resistivity: (a) porosity and density, (b) ultrasonic pulse velocity and dynamic modulus of elasticity, (c) permeability, and (d) unconfined compressive strength. Note: PC = pervious concrete; UPV = ultrasonic pulse velocity; DME = dynamic modulus of elasticity; UCS = unconfined compressive strength.

was similar to the results reported elsewhere, where increasing aggregate content and reduced cement coating corresponded to lower sound absorption ability (24). Furthermore, it is noteworthy to mention that previous investigations conducted on asphalt concrete and cement concrete materials have suggested that mixtures with higher porosities allow for better sound absorption characteristics (lower tire–pavement noise), attributed to their lower EFR compared with the dense-graded mixtures (25, 26, 28).

The relationships between EFR and hardened PC properties are presented through scatter diagrams in Figure 12, a to d. Good-to-excellent correlations were observed between different parameters, where the EFR (characteristic impedance of PC) increased with increasing porosity of the mix and vice versa. Further, higher EFR corresponded to PC with lower permeability and augmented strength. These results are important as they confirm that PC designed with higher air void content will result in lower EFR and ultimately lower noise levels, which corroborates with previous studies conducted on asphalt concrete and cement concrete mixtures (25, 26, 28). Furthermore, the EFR was a better predictor of the hardened PC properties, namely, porosity, permeability, and UCS compared with UPV, as evidenced

from the observed higher coefficients of determination (Figure 12, a to d). Essentially, the EFR parameter was computed using a simple, cost-effective, and nondestructive UPV technique, which displayed excellent potential in predicting the quality of PC mixtures. Note that EFR was highly dependent on the porosity or density of PC mixtures, which is an indirect material acoustic parameter. Thus, the EFR parameter showed great promise for future use in understanding tire–pavement noise characteristics as well.

**Comparison of EFR for Various Paving Materials.** Figure 13 depicts the measured EFR of PC mixtures investigated in this research along with the EFR values for conventional pavement types gathered from the existing literature (25, 26, 28). Note that the upper limits of EFR were used to compare the findings and plot the data to present scenarios that related to the least sound absorption. In addition, Portland cement concrete mixtures of different grades (M10–M30) were also prepared in the laboratory and tested for their UPV and EFR parameters. In general, the UCS of PC mixtures varied between 3 and 28 MPa with slightly higher values reported in some studies. Thus, the comparison of the EFR parameter

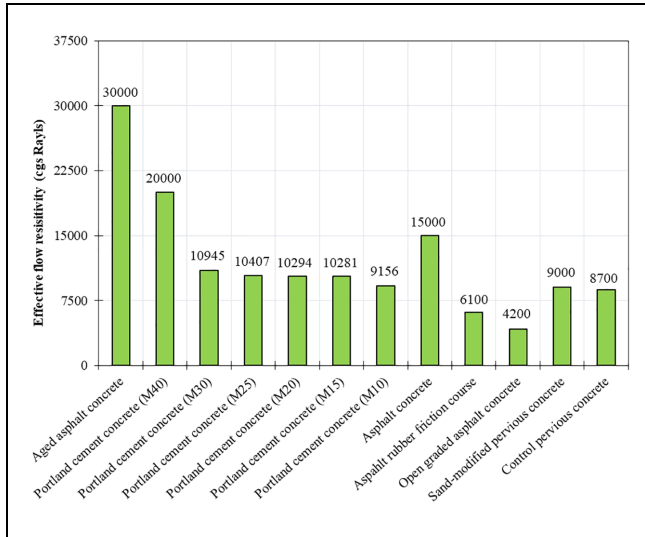


**Figure 13.** Comparison of effective flow resistivity of pervious concrete mixtures and other pavement types.

with cement concrete mixtures of similar grades was deemed essential. As observed, the EFR of PC mixtures was lower than the conventional asphalt concrete and cement concrete pavements. Further, the EFR of asphalt-rubber friction courses and open-graded asphalt concrete surfaces was lower than for PC. These findings are contradictory to the results reported in another study, which indicated that the sound absorption potential of PC was higher than that of the porous asphalt pavements (5). Therefore, the relatively higher EFR values or lower impedance of PC are indicative of dense and strong PC mixtures, which were observed in this research. However, it was interesting to note that the EFRs for all concrete mixtures (M10–M30 grade) prepared in the laboratory were lower than for the PC mixtures, including those with slightly higher strengths, which further revealed that the porous nature of PC can assist in higher noise abatement compared with the traditional concrete. Furthermore, the results showed that though PC mixtures are potential candidates for mitigating the tire–pavement noise, additional efforts must be made to develop mix matrixes that not only allow infiltration of stormwater but also resist vehicular loads while simultaneously assisting in reducing tire–pavement noise.

## Conclusions

This study assessed the suitability of utilizing the nondestructive UPV test method in quantifying the EFR of 36 PC mixtures encompassing three mix variables: (a) four different aggregate sizes; (b) three levels of w/c ratios, and (c) three a/c ratios. The investigation involved the

evaluation of the influence of three mix variables on UPV, DME, and EFR along with investigating the porosity, density, permeability, and compressive strength of hardened PC mixtures, which aided in the development of parametric relationships. The major contributions of this research include:

- The use of the UPV test method to determine the EFR of PC was found to be a promising approach, in that lower EFR was obtained for mixtures with higher porosity and subsequently better sound absorption capacity, and vice versa. Further, EFR was dependent on the aggregate gradation, and lower flow resistivity was obtained for mixtures designed with smaller aggregate particles (6.3–4.75 mm). This was attributed to the increased surface area and presence of a higher number of pores for a given mix volume. Further, sand-modified PC mixtures exhibited higher EFR or greater potential for transmissibility of sound than the control PC owing to their lower air void content.
- The EFR parameter was found to have very good to excellent correlations ( $R^2 \sim 80\%–92\%$ ) with the properties of PC. Indeed, the EFR was a reasonably good predictor of the materials properties compared with UPV, which confirmed that the simplified approach proposed in this study was rational and could be adopted as a nondestructive quality-control test to characterize PC paving mixtures.
- The UCS of sand-modified PC mixtures was notably higher (about 35%–43%) than control PC, with porosity still being above the minimum requirements of 15%, as prescribed by the American Concrete Institute.
- Three-parameter Weibull probability distribution functions were developed and proposed for the computation of both permeability and UCS of PC mixtures.
- The DME of PC varied between 16 and 35 GPa, which was found to be a function of the aggregate gradation and packing.

The findings of this study demonstrated that UPV could be successfully utilized to determine the quality of PC mixtures. As part of the future research, attempts are underway to investigate the influence of transducers with different frequency ranges on the EFR. Additional research must be done to assess the differences in the EFR obtained using the proposed framework and other sophisticated tools that are commonly used. Note that EFR, being the characteristic impedance of a material, provides an indirect assessment of the sound absorption

ability of PC cores without the need for performing a full-scale field evaluation. Furthermore, the application of UPV in predicting the impedance of PC was found to be simple, cost-effective, and scientific, so it has the potential to be a suitable alternative to the other sophisticated instrumentation and analytical techniques. It is envisioned that the UPV test method can be successfully adopted as a nondestructive quality-control toolkit by researchers and practitioners to derive the properties of PC pavements comprising a broad range of mix proportions, pore structure arrangement, porosity levels, and field applications.

### Author Contributions

The authors confirm contribution to the paper as follows: study conception and design: A. Singh, K.P. Biligiri; data collection: A. Singh; analysis and interpretation of results: A. Singh, K.P. Biligiri, P.V. Sampath; draft manuscript preparation: A. Singh, K.P. Biligiri, P.V. Sampath. All authors reviewed the results and approved the final version of the manuscript.

### Declaration of Conflicting Interests

The author(s) declared no potential conflicts of interest with respect to the research, authorship, and/or publication of this article.

### Funding

The author(s) received no financial support for the research, authorship, and/or publication of this article.

### ORCID iDs

Avishreshth Singh  <https://orcid.org/0000-0002-5153-7241>  
 Krishna Prapoorna Biligiri  <https://orcid.org/0000-0002-2313-0815>

### Data Accessibility Statement

All data generated or analyzed during this study are included in this published article.

### References

1. ACI 522. *Report on Pervious Concrete*. American Concrete Institute, Farmington Hills, Michigan, 2010. [https://www.concrete.org/store/productdetail.aspx?ItemID=52210&Format=PROTECTED\\_PDF&Language=English&Units=US\\_AND\\_METRIC](https://www.concrete.org/store/productdetail.aspx?ItemID=52210&Format=PROTECTED_PDF&Language=English&Units=US_AND_METRIC)
2. Chandrappa, A. K., and K. P. Biligiri. Relationships between Structural, Functional, and X-Ray Microcomputed Tomography Parameters of Pervious Concrete for Pavement Applications. *Transportation Research Record*, 2017. 2629(1): 51–62.
3. Singh, A., P. V. Sampath, and K. P. Biligiri. A Review of Sustainable Pervious Concrete Systems: Emphasis on Clogging, Material Characterization, and Environmental Aspects. *Construction and Building Materials*, Vol. 261, 2020, p. 120491.
4. Ong, G. P., and T. F. Fwa. Wet-Pavement Hydroplaning Risk and Skid Resistance: Modeling. *Journal of Transportation Engineering*, Vol. 133, No. 10, 2007, pp. 590–598.
5. Longjia, C., T. F. Fwa., and H. T. Kiang. Laboratory Evaluation of Sound Absorption Characteristics of Pervious Concrete Pavement Materials. *Transportation Research Record: Journal of the Transportation Research Board*, 2017. 2629(1): 91–103.
6. Singh, A., P. Vaddy, and K. P. Biligiri. Quantification of Embodied Energy and Carbon Footprint of Pervious Concrete Pavements through a Methodical Lifecycle Assessment Framework. *Resources, Conservation and Recycling*, Vol. 161, 2020, p. 104953.
7. Singh, A., G. S. Jagadeesh, P. V. Sampath, and K. P. Biligiri. Rational Approach for Characterizing in Situ Infiltration Parameters of Two-Layered Pervious Concrete Pavement Systems. *Journal of Materials in Civil Engineering*, Vol. 31, No. 11, 2019, p. 04019258.
8. Vaddy, P., A. Singh, P. V. Sampath, and K. P. Biligiri. Multi-Scale in Situ Investigation of Infiltration Parameter in Pervious Concrete Pavements. *JTE*, Vol. 49, No. 5, 2020, pp. 3519–3527.
9. ASTM C1688/1688-M. *Test Method for Density and Void Content of Freshly Mixed Pervious Concrete*. ASTM International, West Conshohocken, Pennsylvania, 2014. <http://www.astm.org/cgi-bin/resolver.cgi?C1688C1688M-14A>
10. Rao, Y., Y. Ding, A. K. Sarmah, D. Liu, and P. Pan. Vertical Distribution of Pore-Aggregate-Cement Paste in Statically Compacted Pervious Concrete. *Construction and Building Materials*, Vol. 237, 2020, p. 117605.
11. Kayhanian, M., D. Anderson, J. T. Harvey, D. Jones, and B. Muhunthan. Permeability Measurement and Scan Imaging to Assess Clogging of Pervious Concrete Pavements in Parking Lots. *Journal of Environment Management*, Vol. 95, No. 1, 2012, pp. 114–123.
12. Yu, F., D. Sun, M. Hu, and J. Wang. Study on the Pores Characteristics and Permeability Simulation of Pervious Concrete Based on 2D/3D CT Images. *Construction and Building Materials*, Vol. 200, 2019, pp. 687–702.
13. Lederle, R., and T. Shepard, V. De La Vega Meza. Comparison of Methods for Measuring Infiltration Rate of Pervious Concrete. *Construction and Building Materials*, Vol. 244, 2020, p. 118339.
14. Ridengaoqier, E., and S. Hatanaka. Prediction of Porosity of Pervious Concrete Based on Its Dynamic Elastic Modulus. *Results in Materials*, Vol. 10, 2021, p. 100192.
15. Borhan, T. M., and R. J. Al Karawi. Experimental Investigations on Polymer Modified Pervious Concrete. *Case Studies in Construction Materials*, Vol. 12, 2020, p. e00335.
16. Martins Filho, S. T., E. M. Bosquesi, J. R. Fabro, and R. Peralisi. Characterization of Pervious Concrete Focusing on Non-Destructive Testing. *Revista IBRACON Estruturas Materials*, Vol. 13, 2020, pp. 483–500.
17. Chandrappa, A. K., and K. P. Biligiri. Influence of Mix Parameters on Pore Properties and Modulus of Pervious



- Concrete: An Application of Ultrasonic Pulse Velocity. *Materials and Structures*, Vol. 49, No. 12, 2016, pp. 5255–5271.
18. Amini, K., X. Wang, and N. Delatte. Statistical Modeling of Hydraulic and Mechanical Properties of Pervious Concrete Using Nondestructive Tests. *Journal of Materials in Civil Engineering*, Vol. 30, No. 6, 2018, p. 04018077.
  19. Yap, S. P., P. Z. C. Chen, Y. Goh, H. A. Ibrahim, K. H. Mo, and C. W. Yuen. Characterization of Pervious Concrete with Blended Natural Aggregate and Recycled Concrete Aggregates. *Journal of Cleaner Production*, Vol. 181, 2018, pp. 155–165.
  20. Bérengier, M. C., M. R. Stinson, G. A. Daigle, and J. F. Hamet. Porous Road Pavements: Acoustical Characterization and Propagation Effects. *The Journal of the Acoustical Society of America* Vol. 101, No. 1, 1997, pp. 155–162.
  21. Kim, H. K., and H. K. Lee. Acoustic Absorption Modeling of Porous Concrete Considering the Gradation and Shape of Aggregates and Void Ratio. *Journal of Sound and Vibration*, Vol. 329, No. 7, 2010, pp. 866–879.
  22. Zhong, K. *Research on Properties of Vibration Reduction and Noise Absorption of Porous Concrete Materials*. Masters' thesis. Harbin Institute of Technology, Harbin, China, 2011.
  23. Ni, T. Y., C. H. Jiang, H. X. Tai, and G. Q. Zhao. Experimental Study on Sound Absorption Property of Porous Concrete Pavement Layer. *Applied Mechanics and Materials*, Vol. 507, 2014, pp. 238–241.
  24. Zhang, Y., H. Li, A. Abdelhady, and H. Du. Laboratorial Investigation on Sound Absorption Property of Porous Concrete with Different Mixtures. *Construction and Building Materials*, Vol. 259, 2020, pp. 120414.
  25. Biligiri, K. P., and G. B. Way. Noise-Damping Characteristics of Different Pavement Surface Wearing Courses. *Road Materials and Pavement Design*, Vol. 15, No. 4, 2014, pp. 925–941.
  26. Biligiri, K. P., and K. E. Kaloush. Prediction of Pavement Materials' Impedance Using Ultrasonic Pulse Velocity. *Road Materials and Pavement Design*, Vol. 10, No. 4, 2009, pp. 767–787.
  27. Hastings, A. L. *Traffic Noise Model 3.0: Technical Manual*. Report No.: FHWA-HEP-20-012. Federal Highway Administration, Washington, D. C., 2019. <https://rosap.nsl.bts.gov/view/dot/48763>
  28. Rochat, J. L., and D. R. Read. Effective Flow Resistivity of Highway Pavements. *The Journal of the Acoustical Society of America*, Vol. 134, No. 6, 2013, pp. 4710–4716.
  29. ANSI/ASA S1.18-2010. *American National Standard Method for Determining the Acoustic Impedance of Ground Surfaces*. Acoustical Society of America, New York, 2010. <https://webstore.ansi.org/Standards/ASA/ansiasas1182010>
  30. ASTM C494/C494-M. *Standard Specification for Chemical Admixtures for Concrete*. ASTM International, West Conshohocken, Pennsylvania, 2019.
  31. IS: 2386. *Methods of Test for Aggregates for Concrete (Part 1)—Particle Size and Shape (Reaffirmed 2002)*. Indian Standard, New Delhi, India, 1963.
  32. IS: 12269. *Specification for 53-Grade Ordinary Portland Cement*. Indian Standard, New Delhi, India, 2013.
  33. Singh, A., K. P. Biligiri, and P. V. Sampath. Development of Framework for Ranking Pervious Concrete Pavement Mixtures: Application of Multi-Criteria Decision-Making Methods. *International Journal of Pavement Engineering*, 2022, pp. 1–14.
  34. Singh, A., K. P. Biligiri, and P. V. Sampath. Engineering Properties and Lifecycle Impacts of Pervious All-Road All-Weather Multilayered Pavement. *Resources, Conservation and Recycling*, Vol. 180, 2022, p. 106186.
  35. ASTM 1754/C1754-M. *Test Method for Density and Void Content of Hardened Pervious Concrete*. ASTM International, West Conshohocken, Pennsylvania, 2012. <http://www.astm.org/cgi-bin/resolver.cgi?C1754C1754M-12>
  36. ASTM C597. *Standard Test Method for Pulse Velocity through Concrete*. ASTM International, West Conshohocken, Pennsylvania, 2016.
  37. Singh, A. Development of Pervious All-Road Class All-Weather Multilayered Paver (PARAMpave) Blocks. PhD dissertation. Indian Institute of Technology Tirupati, Indian, 2021.
  38. ASTM C39. *Standard Test Method for Compressive Strength of Cylindrical Concrete Specimens*. ASTM International, West Conshohocken, Pennsylvania, 2021.
  39. Ibrahim, A., E. Mahmoud, M. Yamin, and V. C. Patibandla. Experimental Study on Portland Cement Pervious Concrete Mechanical and Hydrological Properties. *Construction and Building Materials*, Vol. 50, 2014, pp. 524–529.
  40. Pereira da Costa, F. B., L. M. Haselbach, and L. C. P. Da Silva Filho. Pervious Concrete for Desired Porosity: Influence of w/c Ratio and A Rheology-Modifying Admixture. *Construction and Building Materials*, Vol. 268, 2021, p. 121084.
  41. Huang, B., H. Wu, X. Shu, and E. G. Burdette. Laboratory Evaluation of Permeability and Strength of Polymer-Modified Pervious Concrete. *Construction and Building Materials*, Vol. 24, No. 5, 2010, pp. 818–823.
  42. Kevern, J. T., D. Biddle, and Q. Cao. Effects of Macrosynthetic Fibers on Pervious Concrete Properties. *Journal of Materials in Civil Engineering*, Vol. 27, No. 9, 2015, p. 06014031.
  43. Deo, O., and N. Neithalath. Compressive Behavior of Pervious Concretes and A Quantification of the Influence of Random Pore Structure Features. *Materials Science and Engineering: A*, Vol. 528, No. 1, 2010, pp. 402–412.
  44. Zhang, Y., H. Li, A. Abdelhady, and J. Yang. Effect of Different Factors on Sound Absorption Property of Porous Concrete. *Transportation Research Part D: Transport and Environment* Vol. 87, 2020, p. 102532.
  45. Ngohpok, C., V. Sata, T. Satiennam, P. Klungboonkrong, and P. Chindaprasirt. Mechanical Properties, Thermal Conductivity, and Sound Absorption of Pervious Concrete Containing Recycled Concrete and Bottom Ash Aggregates. *KSCE Journal of Civil Engineering*, Vol. 22, No. 4, 2018, pp. 1369–1376.